Stringent upper limits of minor species at the cloud top of Venus: PH3, HCN, and NH3

T. Encrenaz, T. K. Greathouse, R. Giles, T. Widemann, B. Bézard, Franck Lefèvre, Maxence Lefevre, W. Shao, H. Sagawa, Emmanuel Marcq, et al.

A&A, 690, A304 (2024)
https://doi.org/10.1051/0004-6361/202451495

Astronomy & Astrophysics

Stringent upper limits of minor species at the cloud top of Venus: PH_3, HCN, and NH_3

T. Encrenaz[1,⋆], T. K. Greathouse[2], R. Giles[2], T. Widemann[1], B. Bézard[1], F. Lefèvre[3], M. Lefèvre[3], W. Shao[4], H. Sagawa[5], E. Marcq[3], and A. Arredondo[2]

[1] LESIA, Observatoire de Paris, PSL Université, CNRS, Sorbonne Université, Université de Paris, 92195 Meudon, France
[2] SwRI, Div. 15, San Antonio, TX 78228, USA
[3] LATMOS/IPSL, UVSQ Université Paris-Saclay, Sorbonne Université, CNRS, 78280 Guyancourt, France
[4] Denmark Technical University, 2800 Kongens Lyngby, Denmark
[5] Kyoto Sangyo University, Kyoto 603-8555, Japan

Received 13 July 2024 / Accepted 13 September 2024

ABSTRACT

Aims. Following several reports announcing the detection or non-detection of minor species above the clouds of Venus, we have searched for other possible signatures of PH_3, HCN, and NH_3 in the infrared range.
Methods. Since 2012, we have performed ground-based observations of Venus in the thermal infrared at various wavelengths to monitor the behavior of SO_2 and H_2O at the cloud top. We have identified spectral intervals where transitions of PH_3 (around 955 cm^{-1}), HCN (around 747 cm^{-1}), and NH_3 (around 951cm^{-1}) are present.
Results. From the absence of any feature at these frequencies, we derive, on the disk-integrated spectrum, a 3-σ upper limit of 3 ppbv for the PH_3 mixing ratio, 0.5 ppbv for HCN, and 0.3 ppbv for NH_3, assuming that these species have a constant mixing ratio throughout the atmosphere. Maps of the Venus disk recorded at the center position of the lines show that there is no evidence for local detection anywhere over the Venus disk.
Conclusions. Our results bring new constraints on the maximum abundance of these species at the cloud top and in the lower mesosphere of Venus.

Key words. planets and satellites: atmospheres – planets and satellites: composition – planets and satellites: terrestrial planets

1. Introduction

The atmospheric chemistry of Venus is driven by the cycles of water and sulfur dioxide (Krasnopolsky 1986, 2007, 2010; Mills et al. 2007; Zhang et al. 2012). These cycles have been extensively monitored over several decades, using Pioneer Venus, the Venera 15 spacecraft, Venus Express, and Akatsuki, via imaging and spectroscopy in the ultraviolet and infrared ranges. More recently, the SOIR infrared spectrometer aboard Venus Express, working in solar and stellar occultation modes, provided a large dataset regarding the atmospheric composition of Venus above the clouds (Vandaele et al. 2017a,b; Marcq et al. 2020; Mahieux et al. 2023).

In September 2020, the detection of phosphine (PH_3) on Venus was reported on the basis of millimeter heterodyne spectroscopy measurements (Greaves et al. 2020). This result is a big surprise, as the presence of phosphine is not expected in an oxidized atmosphere, such as those of the terrestrial planets, if abiotic processes only are considered. Although questioned by independent reanalyses of the data leading to negative results (Snellen et al. 2020; Thompson 2021; Villanueva et al. 2021), this announcement has fueled interest in the search for minor species in the mesosphere of Venus. Mogul et al. (2021) have published a reanalysis of data recorded by the Pioneer Venus Large Probe Neutral Mass Spectrometer (LPNMS), in which they report the detection of PH_3 and other minor species within the clouds (z = 51 km). Using SOIR, 3-σ upper limits are reported for PH_3 (0.2 ppbv at 65 km, Trompet et al. 2021) and for several other minor species (H_2CO, O_3, NH_3, HCN, N_2O, NO_2, NO, and HO_2 (HCN < 2.5 ppbv at 62 km and NH_3 < 0.2 ppbv at 65 km; Mahieux et al. 2024).

Since 2012, we have been monitoring the abundances of SO_2 and H_2O – by observing monodeuterated water HDO as a proxy – using ground-based imaging spectroscopy in the thermal infrared range with the TEXES (Texas Echelon Cross Echelle Spectrograph) imaging spectrometer, mounted at the Infrared Telescope Facility at Maunakea Observatory (Encrenaz et al. 2023). This facility allows us to probe the atmosphere of Venus in the vicinity of the cloud top (in our model, the cloud top corresponds to an altitude of 62 km) and is thus well suited for the study of minor species at this altitude range. It is thus complementary to the observations by SOIR, which, using the solar-stellar occultation technique, probes above the cloud top (z = 65–100 km). Using a spectrum taken on March 28, 2015, from our previous database, we published a 3-σ upper limit of 5 ppbv for the PH_3 mixing ratio at the cloud top (Encrenaz et al. 2020, hereafter, E20). In July 2023, we obtained new maps of Venus in two different spectral intervals around 955 cm^{-1} and 747 cm^{-1}, in order to search for PH_3 and HCN, respectively. In addition, we searched for previous spectra around 951 cm^{-1}, in order to retrieve an upper limit of the NH_3 mixing ratio. Indeed, HCN and NH_3 are among the species that were tentatively detected by the Pioneer Venus LPNSM (Mogul et al. 2021) and are important minor species in the chemistry of Venus' atmosphere.

In this paper, we first describe the observations from July 2023 (Section 2). Abundance upper limits at the cloud top of

⋆ Corresponding author; therese.encrenaz@obspm.fr

Table 1. Spectroscopic parameters of the molecular transitions used in this study, extracted from the GEISA-2020 database: PH_3 at 955.2 cm^{-1}, HCN at 747.4 cm^{-1}, and NH_3 at 951.8 cm^{-1}.

Species	Wavenumber (cm^{-1})	Band identification	Line identification	Intensity ($cm\ molec^{-1}$)	Energy (cm^{-1})	Broad. coef. ($cm^{-1}\ atm^{-1}$)
PH_3	955.23186	0100 0000	3 2 0E 4 2 0E	1.02×10^{-20}	86.8739	0.0744
CO_2	955.306951	000 11 100 01	P11E	6.663×10^{-27}	1426.0243	0.0807
HCN	747.407040	0 1 1 0 0 0 0 0	R 11	2.108×10^{-19}	195.0747	0.1002
CO_2	747.353675	2 0 0 02 1 1 1 02	Q22F	6.461×10^{-26}	2094.8606	0.0711
CO_2	747.379179	1 1 1 01 0 2 2 01	R19F	1.98×10^{-26}	1474.2336	0.0724
NH_3	951.776242	0100 00 0 A1′ 0000 00 0 A2″	1 0 s A2′ A2′ 0 0 a A1′ A2″	1.613×10^{-19}	0.7934	0.1037
CO_2	951.641607	0 1 1 11 1 1 1 01	R36F	2.3×10^{-25}	2597.8979	0.0681

Notes. The nearby CO_2 transitions were also added. The line intensities correspond to a temperature of 296 K. The broadening coefficients (HWHM) refer to air-broadening.

Venus are presented for PH_3 (Section 3) and HCN (Section 4). In Section 5, we present the NH_3 upper limit retrieved from our archive data. Our results are discussed in Section 6.

2. July 2023 observations

TEXES is an imaging high-resolution thermal infrared spectrograph in operation at the NASA Infrared Telescope Facility at Maunakea Observatory, Hawaii (Lacy et al. 2002). It operates between 5 and 25 μm, and combines high spectral capabilities (R = 80 000 at 7 μm) and spatial capabilities (around 1 arcsec).

Data were recorded in July 2023, in two spectral ranges corresponding to two transitions of PH_3 and HCN, respectively. The Venus diameter was 42 arcsec, with 19% illumination, and the evening terminator was observed. We focused on the PH_3 transition at 955.23 cm^{-1} (already analyzed previously, see E20 and Table 1), and on the HCN transition at 747.408 cm^{-1}. Two spectral ranges were recorded, at 952–957.5 cm^{-1} for PH_3 and at 744–748 cm^{-1} for HCN. The Doppler velocity was −11 km/s, corresponding to a Doppler shift of + 0.035 cm^{-1} at 955 cm^{-1} and + 0.027 cm^{-1} at 747 cm^{-1}. At 950 cm^{-1}, the slit length was 8 arcsec and the slit width was 1.4 arcsec; at 747 cm^{-1}, the slit length was 10 arcsec and its width was 1.3 arcsec. We aligned the slit along the north-south celestial axis, and we shifted it from west to east, with a step of half the slit width and an integration time of 2 seconds per position, to cover the planet in longitude from limb to limb and to add a few pixels on the sky beyond each limb for sky subtraction. The atmospheric transmission is very good around 950 cm^{-1}; a single broad feature is observed at 955.25 cm^{-1} (rest frequency) due to terrestrial atmospheric water vapor. The Doppler-shifted line lies at 955.22 cm^{-1}, close to the position of the PH_3 transition. The atmospheric transmission is good in the vicinity of the HCN transition, between 747.3 and 747.8 cm^{-1}.

The TEXES data cubes were calibrated using the standard radiometric method (Lacy et al. 2002; Rohlfs & Wilson 2004). Calibration frames consisting of black chopper blade measurements and sky observations were systematically taken before each observing scan, and the difference (black minus sky) was taken as a flat field. If the temperature of the black blade, the telescope, and the sky are equal, this method corrects both telescope and atmospheric emissions.

3. PH_3 upper limit

Figure 1 shows the disk-integrated spectrum of Venus between 955.0 and 955.4 cm^{-1}, before and after correction from the terrestrial atmospheric opacity. The atmospheric opacity was recorded for each pixel by the TEXES instrument, and the correction was achieved by dividing the disk-integrated raw spectrum of Venus by the disk-integrated atmospheric transmission spectrum. Two CO_2 transitions appeared at 955.31 and 955.36 cm^{-1} (Table 1). They were used to validate our atmospheric model. As in our earlier PH_3 analysis (E20), we used the line-by-line radiative transfer code which has been used to monitor the variations in SO_2 and HDO at the cloud top of Venus (Encrenaz et al. 2013, 2023), and we adjusted the atmospheric parameters to fit the two CO_2 transitions. In the model inferred from our CO_2 retrieval, the cloud top, at 62 km, has a pressure of 136 mbars and a temperature of 235 K. At an altitude of 80 km, the pressure is 3.1 mbar and the temperature is 198 K. We assumed for PH_3 (as for HCN and NH_3) a constant mixing ratio as a function of altitude, as was also done by Greaves et al. (2020) and Trompet et al. (2021). The spectroscopic data for CO_2 and the minor species discussed in this paper are shown in Table 1. For the broadening coefficients of PH_3, HCN, and

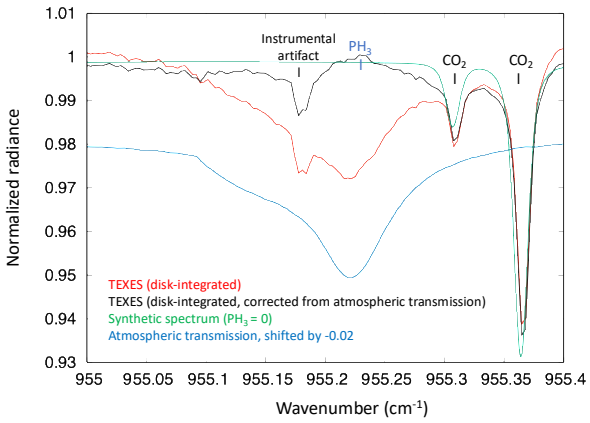

Fig. 1. Disk-integrated TEXES spectrum recorded on July 16, 2023, between 955.0 and 955.4 cm^{-1} (red curve). The total error bar corresponds to a 3σ uncertainty. The broad absorption feature around 955.22 cm^{-1} is due to a telluric water vapor line. The black curve shows the Venus spectrum, divided by the atmospheric transmission. The feature at 955.18 cm^{-1} is an artifact, due to an overlap between two consecutive orders; it was not present in the data of March 2015, due to a different instrumental setting. Green curve: Synthetic spectrum including CO_2 only. The blue curve is the atmospheric transmission, as measured by the TEXES instrument. The slight emission of the corrected TEXES spectrum near the center of the terrestrial absorption line might suggest a slight overcorrection of the atmospheric absorption.

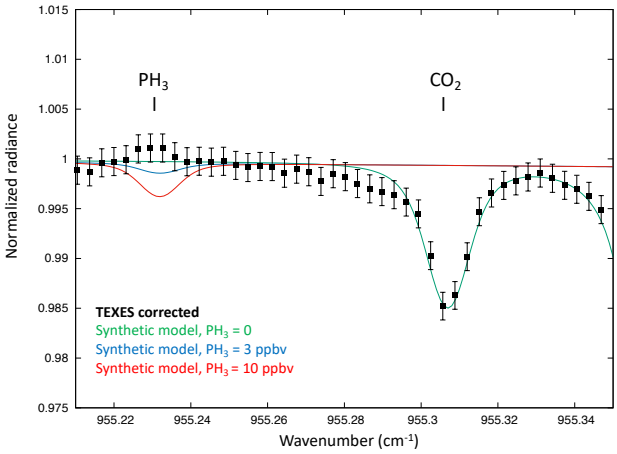

Fig. 2. Disk-integrated TEXES spectrum of Venus (black points) recorded on July 16, 2023, between 955.21 and 955.35 cm^{-1}, corrected from the terrestrial atmospheric absorption. Models: Synthetic spectra including CO_2 (green curve), PH_3 (3 ppbv, blue curve), and PH_3 (10 ppbv, red curve).

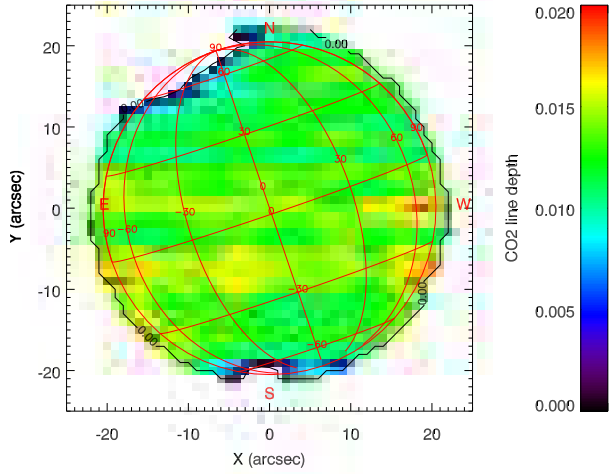

Fig. 3. Map of the line depth of the CO_2 transition at 955.3069 cm^{-1}, recorded on July 16, 2023, corresponding to the spectrum shown in Figures 1 and 2. The low value at high northern latitudes is due to the fact that, in the polar collar, the temperature vertical profile becomes isothermal.

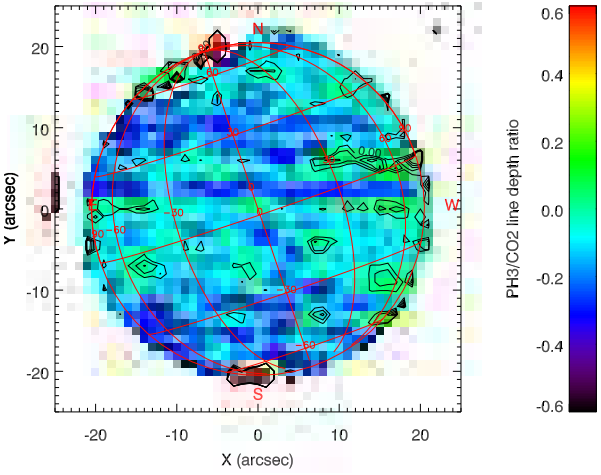

Fig. 4. Map of the PH_3/CO_2 line depth ratio, corresponding to the observation of July 16, 2024. The high values observed at the poles are artifacts (see Figure 3).

NH_3 by CO_2, in the absence of more precise information, we assumed, as we did for SO_2 and HDO (Encrenaz et al. 2016), an increase by a factor of 1.4 with respect to the air-broadening coefficients (Nakazawa & Tanaka 1982).

Figure 2 shows an enlargement of the spectrum in the region where the PH_3 transition is expected. The peak-to-peak (3-σ) variations of the spectrum measured from the fluctuations of the signal outside the lines were estimated to be 0.003 (which corresponds to a 1-σ- signal-to-noise of 1000). As in previous studies, we inferred the volume mixing ratio (vmr) of a minor species by comparing its line depth to that of a weak neighboring CO_2 line; the validity of this method is discussed in earlier papers (Encrenaz et al. 2005, 2012). In the present case, we used the weak CO_2 line at 955.31 cm^{-1} (Table 1). As shown in Figure 2, a line depth of 0.003 corresponds to a PH_3 vmr of 3 ppbv. We noted that the continuum shows a slight emission feature at the position of the PH_3 line, so one could wonder if this might be due to a PH_3 line emission, corresponding to a vmr of 3 ppbv. However, as we are looking at a disk-integrated spectrum, the temperature profile above the cloud top cannot exhibit an inversion, we ruled out this possibility. The slight emission feature might be the result of an overcorrection of the atmospheric opacity.

As in our previous study (E20), we searched for possible variations of the signal over the disk of Venus at the position of the PH_3 transition. The idea was to see if a local emission at the PH_3 line position might appear at a specific location, which could be diluted and not detectable in the disk-integrated spectrum shown in Figures 1 and 2. We defined the depth of this potential PH_3 line by dividing the signal at the line center by the mean value of the continuum on each side of the line, and we mapped this quantity over the disk. Then we mapped the depth of the CO_2 nearby line located at 955.3069 cm^{-1}, and we divided both maps, in order to obtain a map of the PH_3 upper limit over the disk. The results are shown in Figures 3 and 4. We can see from Figure 4 that the PH_3/CO_2 line depth ratio is lower than 0.2 everywhere over the disk. The CO_2 line depth is more or less uniform over the disk, with a mean value of 0.015, as shown in Figure 2. The PH_3 line depth is thus lower than 0.003, which corresponds to an upper limit of 3 ppbv everywhere on the disk for the PH_3 vmr.

4. HCN upper limit

Figure 5 shows the disk-integrated TEXES spectrum recorded between 743.31 and 747.75 cm^{-1}, compared with a spectrum of the terrestrial atmospheric transmission and an atmospheric model of Venus for which, at the cloud top, the pressure is 150 mbar and the temperature is 235 K. It can be seen that the terrestrial atmosphere is clear in this spectral range. All absorption lines are due to CO_2, and the models gives a good overall fit of the various CO_2 transitions. We thus adopt this model to calculate the synthetic spectrum of HCN.

The HCN line we are looking for is at 747.407 cm^{-1} (Table 1), in a region where the continuum of the TEXES spectrum is flat. The peak-to-peak fluctuations of the signal were estimated to be 0.001 (σ = 0.0003). Figure 6 shows the TEXES spectrum of Venus in the 747.395–747.420 cm^{-1} spectral range compared to synthetic models of Venus including absorption by CO_2 and HCN with various mixing ratios. From Figure 6, we infer for HCN a 3σ upper limit of 0.5 ppbv at the cloud top of the Venus atmosphere.

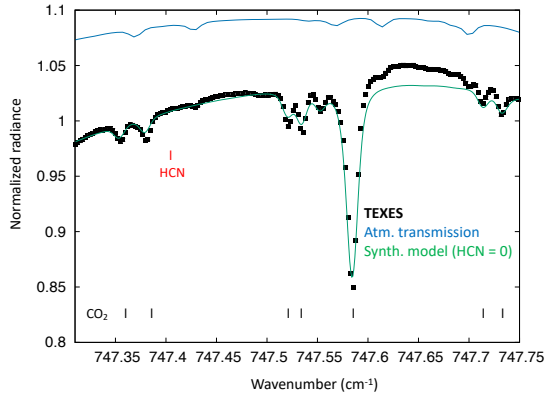

Fig. 5. Disk-integrated TEXES spectrum of Venus (black points) recorded on July 15, 2023, between 747.31 and 747.75 cm^{-1}. Blue curve: Terrestrial atmospheric transmission. Green curve: The synthetic spectrum of Venus. It can be seen that all absorption lines are due to CO_2.

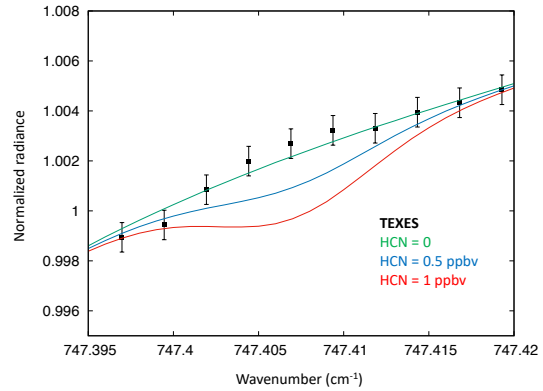

Fig. 6. Disk-integrated spectrum of Venus between 747.395 and 747.420 cm^{-1} recorded on July 15, 2023 (black error bars, (3σ). The models used were CO_2 and HCN, with 0 ppbv (green), 0.5 ppbv (blue), and 1 ppbv (red). The slope of the TEXES spectrum is due to a strong CO_2 transition centered at 746.8 cm^{-1}.

We mapped the signal at the position of the HCN transition to see if HCN might be detectable in a localized spot of the disk. As in the case of PH_3, we divided the signal at the line center position by the mean value of the continuum on each side of the line. Then we mapped the CO_2 neighboring line at 747.3536 cm^{-1} (Fig. 7) and we divided both maps (Fig. 8). It can be seen that the mean line depth ratio is slightly negative, which illustrates that the continuum at the HCN line center is slightly above its value on each side of the line. It can be seen that the variations of the line depth ratio are lower than 0.2 everywhere over the disk. The CO_2 line depth is 0.010 (Fig. 7). The HCN line depth is thus lower than 0.002, which corresponds to an upper limit of HCN of 0.5 ppbv everywhere over the disk.

5. NH_3 upper limit

In the case of NH_3, we selected a strong transition near 951.6 cm^{-1} (Table 1), which happened to be present in two spectra extracted from our TEXES database. This spectral interval was recorded with the purpose of analyzing the CO_2 lines for temperature retrieval. The first spectrum was taken on March 28, 2015, and was previously used for our PH_3 analysis (E20). The Venus diameter was 14 arcsec and the evening terminator

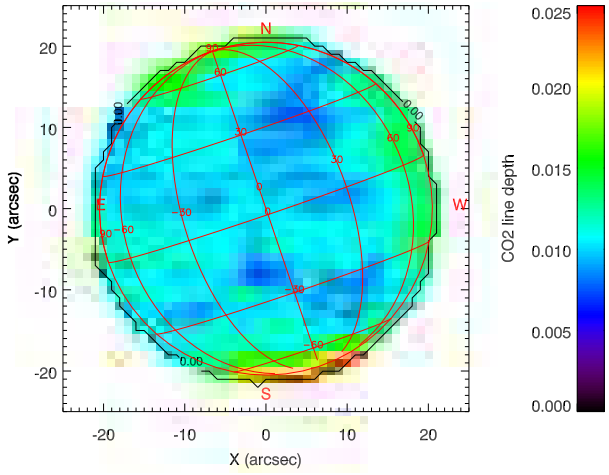

Fig. 7. Map of the CO_2 line depth at 747.35 cm^{-1}, corresponding to the observation of July 15, 2024.

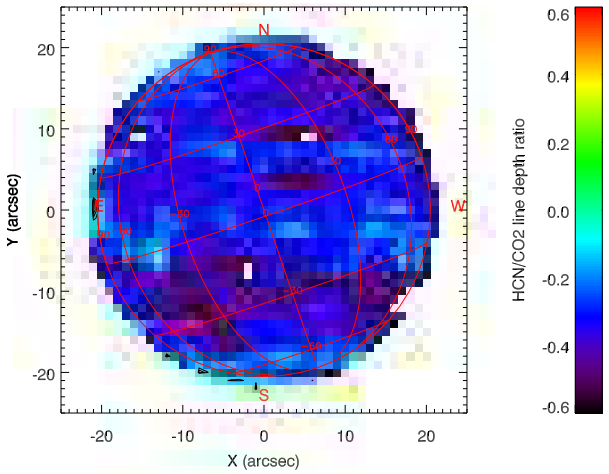

Fig. 8. Map of the HCN/CO_2 line depth ratio, corresponding to the observation of July 23, 2024. The three white spots inside the map correspond to instrumental artifacts.

was observed. The Doppler velocity was –11 km/s, corresponding to a Doppler shift of +0.035 cm^{-1} at 950 cm^{-1}. The second spectrum was taken on January 21, 2016. The diameter of Venus was 13 arcsec and the morning terminator was observed. The Doppler velocity was +9.7 km/s, corresponding to a Doppler shift of –0.031 cm^{-1} at 950 cm^{-1}.

Figure 9 shows the TEXES spectra of March 28, 2015, and January 21, 2016, between 951.55 and 951.85 cm^{-1}. The terrestrial atmospheric transmission is also shown, with a synthetic model of CO_2. A synthetic spectrum of NH_3, with a mixing ratio of 1 ppbv, indicates the position of the NH_3 transition. It can be seen that the terrestrial atmospheric transmission is completely flat in this spectral range, and that the continuum of the TEXES spectra is also flat in the vicinity of the NH_3 transition. Our synthetic spectrum, adjusted to fit the CO_2 transition at 951.64 cm^{-1}, was calculated assuming a pressure of 165 mbar at the T = 235 K level. Figures 10 and 11 show an enlargement of the TEXES spectra in the close vicinity of the NH_3 transition. The peak-to-peak (3 σ) variations of the continuum are estimated to be 2 10^{-3}, corresponding to a σ S/N of 1500. From Figures 10 and 11, we derive a disk-integrated 3σ upper limit of 0.3 ppbv for NH_3, on both March 28, 2015, and January 21, 2016.

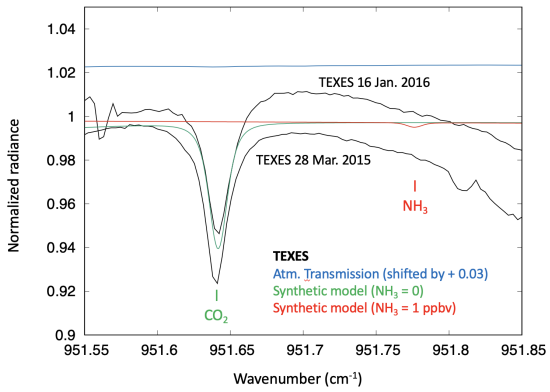

Fig. 9. Disk-integrated TEXES spectrum of Venus (black points) between 951.55 and 951.85 cm^{-1}. Top: January 16, 2016; bottom: March 28, 2015. Green curve: The synthetic spectrum of Venus including the CO_2 line at 951.64 cm^{-1}. The blue horizontal line is the terrestrial atmospheric transmission, shifted by 0.03. Red curve: the synthetic spectrum of Venus including the NH_3 line at 751.776 cm^{-1} with a vmr of 1 ppbv.

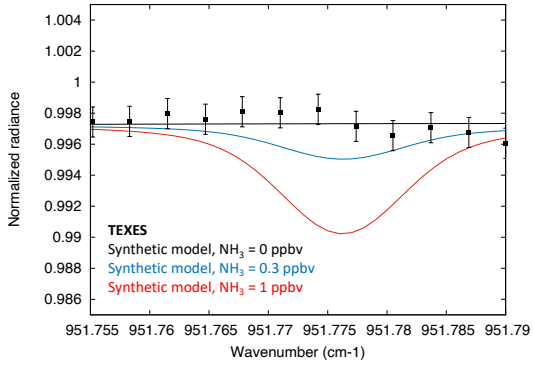

Fig. 10. Disk-integrated spectrum of Venus between 951.755 and 951.790 cm^{-1} recorded on March 28, 2015 (black error bars, 3σ). The models used were NH_3 = 0 ppbv (black curve), 0.3 ppb (blue curve), and 1 ppb (red curve).

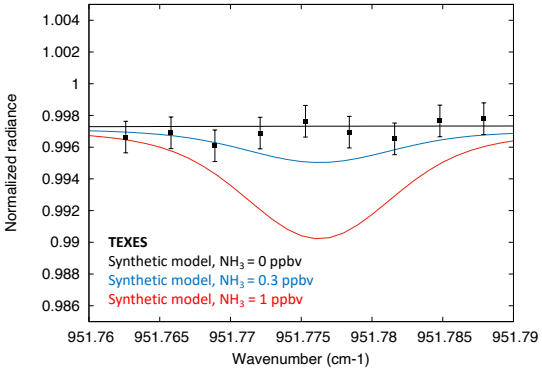

Fig. 11. Disk-integrated spectrum of Venus between 951.760 and 951.790 cm^{-1} recorded on January 16, 2016 (black error bars, 3σ). The models used were NH_3 = 0 ppbv (black curve), NH_3 = 0.3 ppb (blue curve), and NH_3 = 1 ppb (red curve).

Maps of the CO_2 line depth at 951.64 cm^{-1} are shown in Figures 12 and 13 for March 28, 2015, and January 21, 2016, respectively. The low signal (close to zero) at high latitude is a consequence of a change in the temperature profile, which becomes close to isothermal in the polar collars at high latitude

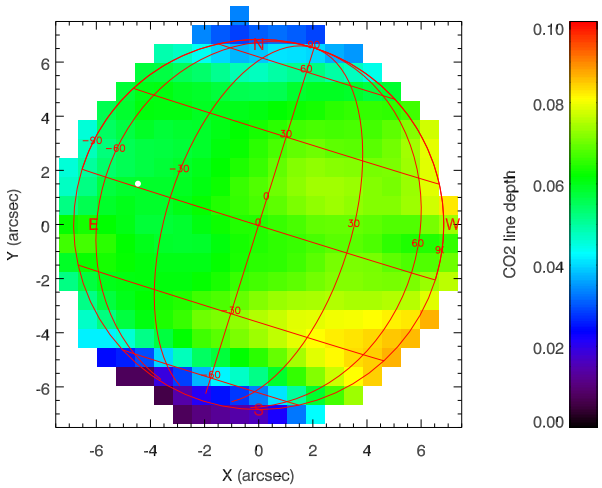

Fig. 12. Map of the line depth of the weak CO_2 transition at 955.3069 cm^{-1}, corresponding to the observations of March 28, 2015, shown in Figures 9 and 10. The subsolar point is shown as a white dot. The negative values in the map of the CO_2 line depth (top) indicate a different behavior of the temperature profile at the level of the polar collar at high latitudes.

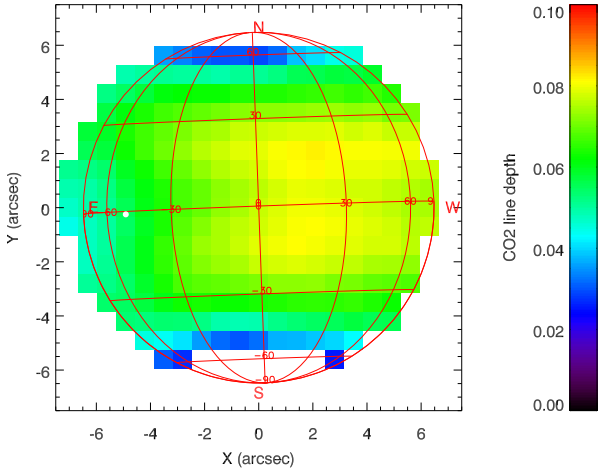

Fig. 13. Map of the line depth of the weak CO_2 transition at 955.3069 cm^{-1}, corresponding to the observation of January 16, 2016, shown in Figures 9 and 11. The change in the temperature profile, at both northern and southern high latitudes, is more pronounced than in March 2015 because the morning terminator is observed.

(Encrenaz et al. 2013). Figures 14 and 15 show the corresponding maps of the pseudo NH_3/CO_2 line depth ratios on March 28, 2015, and January 21, 2016, respectively. The 2015 map is very homogeneous; we inferred an upper limit of 0.1 for the NH_3/CO_2 line depth ratio, which corresponds to an upper limit of 0.006 for the NH_3 line depth, hence a NH_3 upper limit of 1 ppbv. The 2016 map (Fig. 15) is more surprising. The enhancement at high southern latitudes is probably not significant, as the temperature profile is close to isothermal and the line depth ratio is meaningless. We notice that there is a slight increase in the signal from east to west, for which we have no explanation. As in the case of the 2015 map, we find that the NH_3/CO_2 line depth ratio is lower than 0.1. As the CO_2 line depth is 0.06 (Figs. 12 and 13), the NH_3 line depth is thus lower than 0.006. As shown in Figures 9 and 10, a NH_3 vmr of 0.3 ppbv corresponds to a line depth of

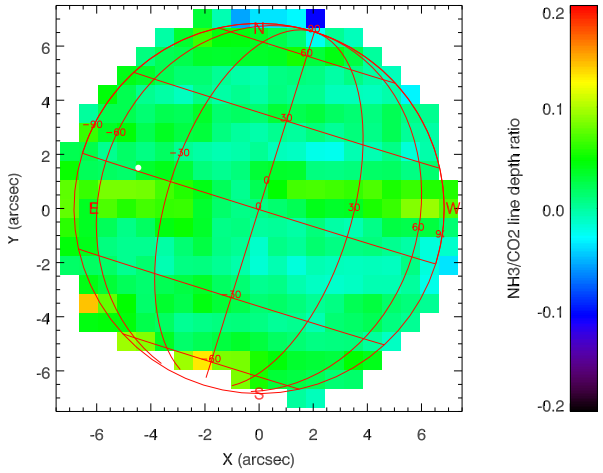

Fig. 14. Map of the NH_3/CO_2 line depth ratio, corresponding to the observation of March 28, 2015.

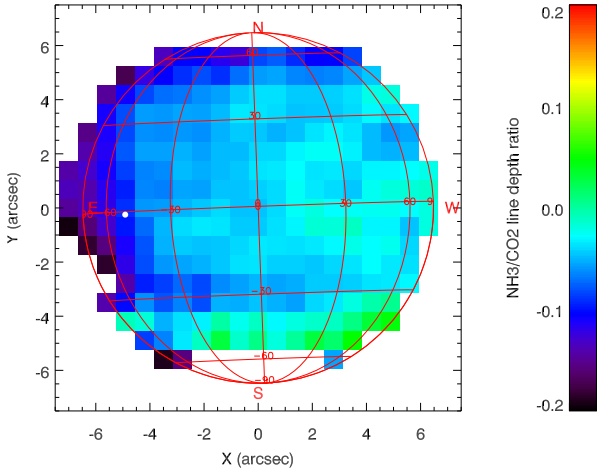

Fig. 15. Map of the NH_3/CO_2 line depth ratio, corresponding to the observation of January 16, 2016.

0.002, and hence the NH_3 vmr is lower than 1 ppbv everywhere on the Venus disk, on both March 28, 2015, and January 16, 2016.

6. Discussion

6.1. PH_3

Greaves et al. (2020) reported the detection of PH_3 in the mesosphere of Venus from two independent submillimeter measurements recorded in 2017 at the *James Clerk Maxwell* Telescope (JCMT) and in 2019 with the Atacama Large Millimeter Array (ALMA), using the 1–0 rotational transition of PH_3 at a wavelength of 1.123 mm. The reported PH_3 vmr was as high as 20 ppbv at an altitude of about 80 km, assuming a constant mixing ratio over the altitude. However, this result was strongly questioned based on independent analyses of the data (Snellen et al. 2020; Thompson 2021; Villanueva et al. 2021); in addition, stringent upper limits of PH_3 were retrieved from thermal infrared ground-based spectroscopic measurements (E20) and from solar occultation measurements by SOIR aboard the Venus Express probe (Trompet et al. 2021). Cordiner et al. (2022), using the GREAT heterodyne spectroscopy instrument aboard the Stratospheric Observatory for Infrared Astronomy (SOFIA), derived a PH_3 upper limit of 0.8 ppbv over altitudes of 75–110 km from the J = 4–3 and J = 2–1 PH_3 transitions, at frequencies near 1 THz and 0.5 THz, respectively. However, using the same dataset but a different reduction treatment, Greaves et al. (2023) inferred a PH_3 vmr of about 1 ppbv. In addition, the authors claimed that the different detection and upper limits could be reconciled if the PH_3 abundance in the mesosphere is governed by photochemistry, with the PH_3 mixing ratio being as high as 20 ppbv in the morning and around 1 ppbv in the evening. However, the data reduction method used by Greaves et al. (2023) was again questioned by Cordiner et al. (2023), who confirmed their earlier upper limits.

In July 2023, the diameter of Venus was 42 arcsec, and hence most of the disk was in the night side, and the evening terminator of Venus was observed. Thus, our disk-integrated upper limit of 3 ppbv is not in conflict with Greaves's interpretation. However, our PH_3 map shows no evidence of a decrease toward the day (evening) side, which would be expected if PH_3 daily variations could be associated to solar insolation through a photochemical cycle. In addition, our map of March 28, 2015, (E20) includes both the subsolar point and the evening terminator. According to Greaves et al. (2023), we would expect the PH_3 abundance to be maximum around 12:00 LT and decrease toward the evening terminator, whereas our map indicates an upper limit of 3 ppbv everywhere. In summary, our study does not support the PH_3 detection and daily cycle suggested by Greaves et al. (2023).

Mogul et al. (2021) announced the detection of PH_3 from the reanalysis of the Pioneer Venus LPNMS. Assigning PH_3 at the atomic mass 33.997 is difficult because H_2S appears at a very close atomic mass (33.987), and the resolution of the mass spectrometer is not sufficient to separate both species. Using other measurements of associated fragments (PH_2, HS) and isotopologs (PH_2D, HDS), the authors concluded that PH_3 (19 counts) was more abundant than H_2S (4 counts) by a factor of almost five. However, the authors gave no indication regarding the PH_3 mixing ratio at the altitude of 51 km.

Our result on PH_3 is slightly lower than derived in our earlier study (E20) and is complementary to the upper limits inferred by Trompet et al. (2021) using solar occultation spectra in the near infrared range, with the SOIR instrument aboard Venus Express. The SOIR's very sensitive technique led to a set of PH_3 upper limits as low as 0.2 ppbv at an altitude of about 65 km.

6.2. HCN

The tentative detection of hydrogen cyanide HCN (with many minor species) was reported by Mogul et al. (2021), at an altitude of 51 km, from a reanalysis of the Pioneer Venus LPNMS; however, there was no mention of its relative abundance. The reported count number for HCN, at the atomic mass 27.01, was 77, while the count number for PH_3, at the atomic mass 33.99, was 19. Using the solar occultation data of SOIR aboard Venus Express, Mahieux et al. (2024) inferred an upper limit of 38.3 ± 7.9 ppmv at an altitude of 80 km. In their paper, one of the vmr vertical profiles of the HCN upper limit indicates a value of 2.5 ppbv at an altitude of 62 km. Our upper limit at the same altitude level is thus improved by a factor of 10. In addition, our study shows that there is no evidence of HCN anywhere on the Venus disk.

6.3. NH_3

Mogul et al. (2021) suggested the plausible presence of NH_3 from the analysis of the LPNMS signal at an atomic mass of 17.02 (NH_3), 16.02 (NH_2), and 15.01 (NH). However, the major

contribution at these peaks comes from $^{13}CH_4$, $^{12}CH_4$, and $^{12}CH_3$ because methane was used as a calibrant; thus, there is no information about the NH_3 abundance. Mahieux et al. (2024), using SOIR data, inferred an upper limit of 0.69 ± 00.28 ppmv at an altitude of 80 km. The lowest upper limit achieved for NH_3 at 65 km is 0.2 ppbv, which is close to our result.

In summary, the upper limits derived in the present study are consistent with the results reported by Mahieux et al. (2024) and complementary to them. Ground-based measurements allow us to derive quantities or upper limits over the apparent full disk of Venus, while the solar occultation technique provides upper limits that are stringent (with a high signal-to-noise ratio, as it uses the sunlight as an initial source) but very localized, at the terminator (typically a few kilometers in the vertical axis) and for a small portion in latitude. Both techniques are thus needed in the future for better understanding of composition of Venus' atmosphere.

Data availability

The TEXES image cubes used in this paper are archived at the InfraRed Science Archive (IRSA), operated by the Infrared Processing and Analysis Center (IPAC) of the California Institute of Technology (https://irsa.ipac.caltech.edu/frontpage/) and can be downloaded at https://irsa.ipac.caltech.edu/applications/irtf/, specifying the Venus NAIF id 299 and the observing runs 2015A008 (March 2015), 2015B012 (January 2016), and 2023A009 (July 2023). Data are available to the community after a 18-month proprietary period.

Acknowledgements. TE, TKG and RG were visiting astronomers at the NASA Infrared Telescope Facility, which is operated by the University of Hawaii under Cooperative Agreement no. NNX-08AE38A with the National Aeronautics and Space Administration, Science Mission Directorate, Planetary Astronomy Program. We wish to thank the IRTF staff for the support of TEXES observations. This work was supported by the Programme National de Planétologie (PNP) of CNRS/INSU, co-funded by CNES. TKG acknowledges support of NASA Grant NNX14AG34G. TE and BB acknowledge support from CNRS. TW acknowledges support from the University of Versailles-Saint-Quentin and the European Commission Framework Program FP7 under Grant Agreement 606798 (Project EuroVenus). ML acknowledges funding from the European Union's Horizon Europe research and innovation program under the Marie Skłodowska-Curie grant agreement 101110489/MuSICA-V. EM acknowledges support from CNES and ESA for all Venus-related studies.

References

Cordiner, M. A., Villanueva, G. L., Wiesemeyer, H., et al. 2022, Geophys. Res. Lett., 49, e2022GL101055
Cordiner, M. A., Wiesemeyer, H., Villanueva, G. L., et al. 2023, Geophys. Res. Lett., 50, e2023GL106136
Encrenaz, T., Bézard, B., Owen, T., et al. 2005, Icarus, 179, 43
Encrenaz, T., Greathouse, T., Roe, H., et al. 2012, A&A, 543, A153
Encrenaz, T., Greathouse, T. K., Richter, M. J., et al. 2013, A&A, 559, A65
Encrenaz, T., Greathouse, T. K., Richter, M. J., et al. 2016, A&A, 595, A74
Encrenaz, T., Greathouse, T. K., Marcq, E., et al. 2020, A&A, 643, L5
Encrenaz, T., Greathouse, T. K., Giles, R., et al. 2023, A&A, 674, A199
Greaves, J., Richards, A. M. S., Bains, W., et al., 2020, Nat. Astron., https://doi.org/10.1038/s41550-020-1174-4
Greaves, J. S., Pelkowsky, J. J., Richards, A. M. S., et al. 2023, Geophys. Res. Lett., 50, e2023GRL103539
Jacquinet-Husson, N., Armante, R., Scott, N. A., et al. 2016, J. Mol. Spectr. 327, 31
Krasnopolsky, V. A. 1986, Photochemistry of the Atmospheres of Mars and Venus (New York: Springer-Verlag)
Krasnopolsky, V. A. 2007, Icarus, 191, 25
Krasnopolsky, V. A. 2010, Icarus, 209, 314
Lacy, J. H., Richter, M. J., Greathouse, T. K., et al. 2002, PASP, 114, 153
Mahieux, A., Robert, S., Picialli, A., et al. 2023, Icarus, 405, 115713
Mahieux, A., Viscardy, S., Jessup, K., et al. 2024, Icarus, 409, 115862
Marcq, E., Bertaux, J.-L., Montmessin, F., et al. 2013, Nat. Geosci., 6, 25
Marcq, Jessup, K. L., Baggio, L., et al. 2020, Icarus, 335, 11386
Mills, F. P., Esposito, L. W., & Yung, Y. K. 2007, in Exploring Venus as a Terrestrial Planet, Geophysical Monograph Series, 176, 73
Mogul, R., Limaye, S. S., Way, M. L., & Cordova, J. A. 2021, Geophys. Res. Lett., 48, e91327
Nakazawa, T., & Tanaka, M. 1982, JQSRT, 28, 409
Rohlfs, K., & Wilson, T. L. 2004, Tools for Radioastronomy, 4th edn. (Berlin: Springer)
Snellen, I. A. G., Guzman-Ramirez, L., Hogerheijde, et al. 2020, A&A, 644, L2
Thompson, M. A. 2021, MNRAS, 501, L18
Trompet, L., Robert, S., Mahieux, A., et al. 2021, A&A, 645, L4
Vandaele, A.-C., Korablev, O., Belyaev, D., et al. 2017a, Icarus, 295, 16
Vandaele, A.-C., Korablev, O., Belyaev, D., et al. 2017b, Icarus, 295, 1
Villanueva, G. L., Cordiner, M., Irwn, P. G. J., et al. 2021, Nat. Astron., 5, 631
Zhang, K., Liang, M. C., & Mills, F. P. 2012, Icarus, 217, 714